

Effect of stress on the electrical resistivity of semiconducting Ti_2O_3 [†]

H.-L. S. Chen and R. J. Sladek

Department of Physics, Purdue University, West Lafayette, Indiana 47907

(Received 20 June 1977)

The effect of uniaxial compression and hydrostatic pressure on the resistivity of single-crystal Ti_2O_3 samples with different crystallographic orientations has been measured between 77 and 300 K. Our results are explainable in terms of the redistribution of Ti 3d electrons accompanying the stress-induced change of the energy gap between simple valence and conduction bands. Deformation potentials of 2.2 and -1.5 eV are deduced for strains perpendicular and parallel to the c axis, respectively. It is inferred that band shift rather than band broadening occurs at the semiconductor-to-semimetal transition between 400 and 550 K.

I. INTRODUCTION

Interest in the α -corundum structure compound¹ Ti_2O_3 has continued for some time because of the gradual semiconductor-semimetal transition²⁻⁶ which occurs in this material between 400 and 550 K due to the approach and overlap of Ti 3d bands.⁷⁻¹¹ Recent work⁶ has indicated that, in a temperature range below 300 K, Ti_2O_3 is an (almost) intrinsic p -type semiconductor with a small electronic energy gap of 0.11 eV. In addition, $\rho_c/\rho_a \approx 2.5$, where ρ_c and ρ_a are the electrical resistivities parallel to the crystalline c axis and a axis, respectively, and the conductivity of holes is about seven times greater than that of electrons.⁶ Previously⁴ a hole effective mass of $5m_0$ has been deduced from thermopower and Hall-effect measurements on nonstoichiometric Ti_2O_3 .

Although ideas about the nature of the valence and conduction bands have existed for some time,^{9,12} only recently have band calculations^{13,14} been made for Ti_2O_3 . The improved band calculation¹⁴ yields results which agree with soft-x-ray data¹⁵ and optical-reflectivity measurements.¹⁶ However, even this calculation does not produce a gap between valence and conduction bands. The authors of the improved band calculation do show how inclusion of electron-electron interactions could produce a gap.

The calculated bands¹⁴ include a valence-band maximum and a conduction-band minimum at the Γ point in the center of the Brillouin zone. However, these band edges exhibit some degeneracy.

Detailed experimental information about the valence- and conduction-band edges is lacking. Although such information is in principle obtainable from magnetoresistance (MR) measurements,¹⁷ the transverse MR is too small at 77 K and above ($\Delta\rho/\rho_0 \leq 10^{-3}$ at 200 kG)^{5,18} to be useful for investigating the edges of the bands responsible for conduction. (It is true that a large transverse

MR is found at 4.2 K in Ti_2O_3 , but it is probably *not* due to band properties, as was originally suggested,⁵ since recent work¹⁹ indicates that hopping conduction may predominate at low temperatures.)

The purpose of the present work is to obtain new information about the electronic energy bands in Ti_2O_3 which is important for a full understanding of the nature of the semiconductor-to-semimetal transition. To achieve this, we have investigated the effect of uniaxial stress and hydrostatic pressure on the electrical resistivity of oriented single-crystal samples of Ti_2O_3 in the semiconducting region.

Application of stress causes a change of resistivity²⁰

$$\Delta\rho = \underline{\pi} : \underline{\tau} , \tag{1}$$

where $\underline{\pi}$ is the piezoresistivity tensor and $\underline{\tau}$ is the stress tensor. Since Ti_2O_3 has the point-group symmetry $\bar{3}m$, $\underline{\pi}$ in contracted notation is given by²¹

$$\underline{\pi} = \begin{pmatrix} \pi_{11} & \pi_{12} & \pi_{13} & \pi_{14} & 0 & 0 \\ \pi_{12} & \pi_{11} & \pi_{13} & -\pi_{14} & 0 & 0 \\ \pi_{31} & \pi_{31} & \pi_{33} & 0 & 0 & 0 \\ \pi_{41} & -\pi_{41} & 0 & \pi_{44} & 0 & 0 \\ 0 & 0 & 0 & 0 & \pi_{44} & 2\pi_{41} \\ 0 & 0 & 0 & 0 & \pi_{14} & -\pi_{11} - \pi_{12} \end{pmatrix} \tag{2}$$

The signs of the π_{ij} 's are conventional; i.e., compressive stress or pressure is assigned a negative sign so that if such stress causes the resistivity to increase, then the appropriate combination of π_{ij} 's is negative.

We shall determine values for some of the π_{ij} 's, or combinations thereof, which provide direct information about the nature of the edges of the valence and conduction bands.

II. EXPERIMENTAL DETAILS

The single-crystal ingot of Ti_2O_3 used to obtain our samples was grown by personnel in the Purdue National Science Foundation-Materials Research Laboratory Central Crystal Growing Facility using Czochralski-Kyropoulos techniques.^{22,23} The ingot was oriented with x-ray diffraction Laue photographs and cut with a wire saw into rectangular parallelepipeds. Each of these was then cemented onto an adjustable grinding jig, x-ray oriented to within 0.5° of the desired orientation, and ground on a glass plate with #600 grit silicon carbide to yield sample thickness and width each uniform to ± 0.0013 cm. The ends of the sample were lapped flat and perpendicular to the sides. Final sample dimensions were about $10 \times 1.5 \times 1$ mm.

In order to make good electrical contacts, the following procedure was used. Each sample was cleaned with acetone, etched with CP4 (HF: acetic acid: HNO_3 : liquid bromine in the ratios 50:50:80:1), rinsed with soapy water and distilled water, and then cleaned in the vapors of isopropyl alcohol as was the indium used as solder. One current lead was soldered near each end of a $1\text{-cm} \times 1.5\text{-mm}$ face, and two potential leads were soldered near the middle of each $1\text{-cm} \times 1\text{-mm}$ face. Contacts with resistances of a few ohms were obtained.

The samples were mounted in a simple, push-rod apparatus for uniaxial compression measurements²⁴ or in a pressure vessel for hydrostatic measurements. We used uniaxial stresses up to 2×10^8 dyn/cm² and hydrostatic pressures up to 3×10^9 dyn/cm². Above 150 K, hydrostatic pressure was obtained from a fluid pressure generating system²⁴ consisting of an intensifier and motor-driven pump. A precision dial gauge was used to measure the pressure. At 150 K and below, a vessel was used which contained a frozen kerosene-mineral-oil mixture previously pressurized at room temperature.²⁵ Various baths held in a Dewar flask were employed to achieve different temperatures which were determined using a copper-constantan thermocouple whose output was measured with a precision digital voltmeter.

Electrical voltages on the sample were measured potentiometrically while the current was supplied and regulated, to within $\pm 0.005\%$ or better, by a constant current power supply.

For measuring the effects of stress on sample resistivity we used the longitudinal arrangement in which the current and voltage drop, and, in the case of uniaxial compression, the stress, are parallel to the long dimension of the sample. Four kinds of sample orientations were used: sample length parallel either to the a axis ([100]), to the c axis ([001]), or to a direction lying in the mirror

TABLE I. Resistivities (in $\text{m}\Omega$ cm) of Ti_2O_3 at selected temperatures.

T (K)	77	100	125	167	195	273	298
ρ_a	296	82	36	16	11.6	7.7	7.2
ρ_c	590	179	82.5	37.7	27.4	19.5	18.7

plane perpendicular to the a axis which is either 45° or 135° away from the positive c axis.

In order to deduce resistivity changes from the measured voltages we applied appropriate corrections to take into account changes in sample dimensions. The latter were calculated from elastic compliances (S_{ij} 's) deduced from measured elastic constants (C_{ij} 's).²⁶ Corrections for the measured resistivity changes being nonisothermal²⁰ were estimated to be negligible.

We shall report fractional changes in resistivity per unit stress and call them piezoresistances. They are related to the piezoresistivity coefficients π_{ij} as follows. For uniaxial compressive stress $-|X|$, $\Delta\rho/\rho_0|X|$ is equal to $-\pi_{11}/\rho_a$ for $\vec{X} \parallel \vec{a}$, $-\pi_{33}/\rho_c$ for $\vec{X} \parallel \vec{c}$, and

$$-[(\pi_{11} + \pi_{33} + \pi_{13} + \pi_{31} + 2\pi_{44}) \pm (\pi_{14} + 2\pi_{41})]/2(\rho_a + \rho_c)$$

for $\vec{X} \parallel [011]$ and $\vec{X} \parallel [01\bar{1}]$, respectively. For hydrostatic pressure P , $\Delta\rho/\rho_0|P|$ is equal to $-(\pi_{11} + \pi_{12} + \pi_{13})/\rho_a$ when the current \vec{I} is parallel to the a axis, and $-(2\pi_{31} + \pi_{33})/\rho_c$ when $\vec{I} \parallel \vec{c}$. Values for ρ_a and ρ_c at some temperatures are listed in Table I.

III. RESULTS AND DISCUSSION

Our piezoresistance data are plotted versus reciprocal temperature in Figs. 1-4. They can be seen to be almost linearly proportional to $1/T$.

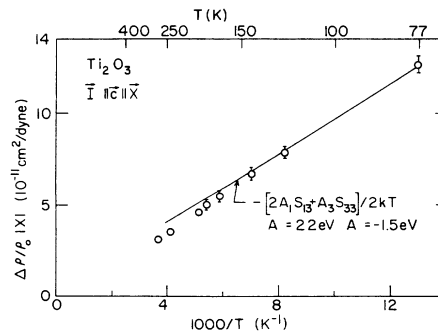


FIG. 1. Piezoresistance data for uniaxial compression, sample length, and current parallel to the c axis plotted versus reciprocal temperature. The solid curve was calculated using Eq. (8) of the text for two simple bands whose change in separation with stress is describable in terms of the deformation potentials A_1 and A_3 .

This behavior is characteristic of the large effects found in semiconductors.²⁰ Hydrostatic pressure data for a *c*-axis sample yield fractional changes of resistivity per unit pressure (π_p) at 273 and 298 K which are about 95% of the values obtained for our *a*-axis sample at corresponding temperatures. (See Fig. 4 for the latter values.) Thus, for $\vec{I} \parallel \vec{c}$, $\pi_p \neq 0$, so that $2\pi_{31} + \pi_{33} \neq 0$. This indicates that a one-band model cannot be appropriate²⁷ for Ti_2O_3 .

Before discussing our other results, we note that there have been some hydrostatic pressure measurements on Ti_2O_3 crystals of unspecified orientation²⁸ yielding larger decreases in resistivity with pressure than those which we obtain. However, the resistivity seems to have been measured as a function of temperature at each of a number of pressures. This method is likely to yield results less accurate than those obtainable by changing the pressure at fixed temperature as we have done above 150 K. In any case, the other hydrostatic pressure work does not give any information about the relative values of π_p for *a*- and *c*-axis samples.

From Fig. 3, it can be seen that $\pi_{011} \approx \pi_{01\bar{1}}$, so that $\pi_{14} + 2\pi_{41} = 0$. (Note that π_{011} and $\pi_{01\bar{1}}$ equal $-\Delta\rho/\rho_0 |X|$ for $[011]$ and $[01\bar{1}]$ length samples, respectively.) This result indicates that the simplest two-band model in which both the valence- and conduction-band edges lie on the k_z axis in momentum space²⁷ is appropriate for Ti_2O_3 . Furthermore, it will turn out that our data are explainable in terms of strain-induced shifts in the separation of the band edges without any change in band shape; i.e., a deformation potential model²⁹ applies. The change in energy gap is given by

$$\Delta E_G = \sum_{i=1}^6 A_i \epsilon_i, \quad (3)$$

where the ϵ_i 's are the components of the strain in contracted notation and the A_i 's are the defor-

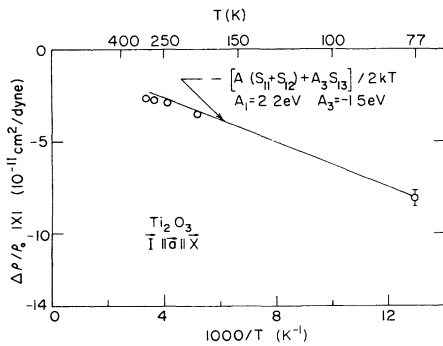


FIG. 2. Same as Fig. 1, except that the *a* axis and Eq. (7) of the text are involved.

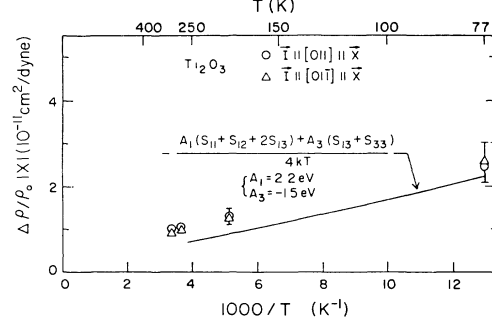


FIG. 3. Same as Fig. 1, except that the directions are 45° between the *b* axis and the positive or negative *c* axis and Eq. (9) of the text is involved.

mation potential constants. In turn, each

$$\epsilon_i = \sum_{j=1}^6 S_{ij} \tau_j,$$

where the S_{ij} are elastic compliances and τ_j are the stress components in contracted notation. For the case of two simple bands²⁷ there are only two independent, nonzero deformation potential constants, $A_1 = A_2$ and A_3 , while $A_4 = A_5 = A_6 = 0$.

Since Ti_2O_3 is a nearly intrinsic semiconductor⁶ in the range of this investigation, the concentration of holes in the valence band, p_v , is approximately equal to the concentration of electrons in the conduction band, n , and each is proportional to $\exp(-E_G/2kT)$. Thus, provided that $\Delta E_G \ll 2kT$,

$$\Delta p/p_0 \approx \Delta n/n_0 \approx -\Delta E_G/2kT \quad (4)$$

(k is Boltzmann's constant, T is absolute temperature). The resistivity tensor is given by

$$\underline{\rho} = 1/\underline{\sigma} = 1/(ne\underline{\mu}_e + pe\underline{\mu}_h), \quad (5)$$

where $\underline{\sigma}$ is the conductivity tensor, and $\underline{\mu}_e$ and $\underline{\mu}_h$

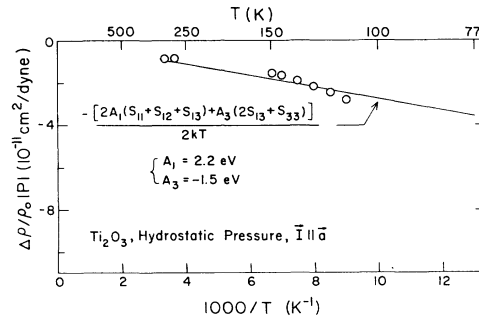


FIG. 4. Piezoresistance due to hydrostatic pressure for sample length and current parallel to the *a* axis plotted versus reciprocal temperature. The solid curve was calculated using Eq. (10) as indicated in the text.

the mobility tensors for electrons and holes, respectively. If the strain dependences of the mobilities are small, then

$$\Delta\rho/\rho_0 \approx \Delta E_G/2kT. \quad (6)$$

For stress $\vec{\tau} \parallel \vec{I} \parallel \vec{a}$, $\tau_1 = -|X| \neq 0$ and τ_2 to $\tau_6 = 0$, where $|X|$ is the magnitude of the uniaxial compressive stress. Thus

$$(\Delta\rho/\rho_0|X|)_a = -[A_1(S_{11} + S_{12}) + A_3S_{13}]/2kT. \quad (7)$$

Similarly, for $\vec{\tau} \parallel \vec{I} \parallel \vec{c}$,

$$(\Delta\rho/\rho_0|X|)_c = -(2A_1S_{13} + A_3S_{33})/2kT. \quad (8)$$

Since the S_{ij} 's (like the C_{ij} 's) are almost independent of temperature³⁰ in the region covered in the present work, Eqs. (7) and (8) indicate that the piezoresistance will be almost proportional to $1/T$ provided that the deformation potentials are constant. Values for A_1 and A_3 can be deduced from Eqs. (7) and (8) by using our experimental piezoresistances and the S_{ij} 's calculated from literature values^{26,30} of the C_{ij} 's.

In addition to the principal effect due to carrier redistribution describable by Eqs. (7) and (8), there might be minor effects which could contribute to the piezoresistances. (For instance, the mobility might be strain dependent.) Various minor effects have been discussed by Keyes²⁰ and by Herring.²⁹ Although there may be a number of minor effects, their contributions to the piezoresistance ordinarily become unimportant at low temperatures because of the proportionality of the principal effect to T^{-1} . Since at the present time there is no accurate way to estimate the magnitude of the minor effects, the experimental uniaxial piezoresistances at 77 K were assumed to be due entirely to carrier redistribution between valence and conduction bands. Thus, using the 77-K values of $\Delta\rho/\rho_0|X|$ in Eqs. (7) and (8), we obtain

$$A_1 = 2.2 \begin{smallmatrix} +0.1 \\ -0.5 \end{smallmatrix} \text{ eV and } A_3 = -1.5 \begin{smallmatrix} +0.1 \\ -0.5 \end{smallmatrix} \text{ eV}.$$

These values are similar to those obtained by Chi and Sladek²⁶ from fitting their elastic constant data (between 300 and 500 K):

$$A_1 = 1.8 \text{ eV and } A_3 = -2.1 \text{ eV}.$$

Our values of the A_i 's are believed to be more reliable because they are obtained quite directly from our experimental data as indicated above. In contrast to this, Chi and Sladek had to choose specific forms for the energy bands and a particular temperature dependence of the energy gap in order to calculate electronic contributions to the elastic constants. These contributions, of course, yield their A_i values. It must be admitted that minor effects might be present to a slight but unknown degree in our data. Our best guess is that

there is a maximum minor-effect contribution of 5% at 77 K which would cause the -0.5 eV error indicated above for each of our A_i 's. Analogous minor effects do not occur in the elastic constants, since the latter do not depend on carrier mobility. However, the elastic constant method depends on the validity of the assumption that the anomalies in the elastic constants in the region of the electrical transition are completely describable as electronic effects. In view of the anomalous behavior of the piezoresistances³¹ in that temperature range, some other mechanism may also be present and contribute to the extrema in the elastic constants, as will be discussed elsewhere. Despite these caveats, it is satisfying that the signs of the A_i 's determined from the two different methods agree. More important is the fact that they are consistent with the c -axis expansion and the a -axis contraction³² as the resistivity decreases with increasing temperature through the electrical transition. This implies that band shift rather than band broadening occurs at the transition.

There has not been any theoretical calculation of the deformation potentials for Ti_2O_3 . Some idea of what would be involved in such an effort is obtainable from papers on Si.³³ From them it can be seen that the problem is to calculate the matrix elements of the perturbation of the Hamiltonian produced by strain. The ingredients for such a calculation—detailed, reliable information about the band structure, the crystal potentials, and the wave functions, etc.—are lacking for Ti_2O_3 . Even in the case of Si for which the band structure and wave functions have been carefully studied and are well known, the calculation of deformation potentials is not easy, because of uncertainty in how strain changes atom positions in a unit cell, the lack of a completely self-consistent band calculation for the strained crystal, and some approximations even in the wave functions of the undeformed state.

It is interesting to compare our deformation potentials for semiconducting Ti_2O_3 with those of the semimetal bismuth because of their common $\bar{3}m$ point-group symmetry and because the energy by which the valence and conduction bands overlap in Bi has a strain dependence describable by two deformation potentials,³⁴ $E_1 = -2.4$ eV and $E_2 = 2.5$ eV. In view of the way E_1 and E_2 are defined and the equivalence of a positive overlap energy to a negative-energy gap, E_1 and E_2 correspond, respectively, to our $-A_1$ and $-A_3$. It can be seen that the values of $-E_1$ and $-E_2$ for Bi are remarkably close to our $A_1 = 2.2$ eV and $A_3 = -1.5$ eV values for Ti_2O_3 . The similarity between the deformation potential values in Ti_2O_3 and Bi is surprising in view of the quite different types of elec-

tronic states involved in electronic transport processes. It should be noted that, unlike Ti_2O_3 , $\pi_{14} + 2\pi_{41} \neq 0$ for Bi,³⁵ which has a multivalley conduction band, a hole band located away from the Γ point, and another close-by hole band.³⁶

Now we shall use the values of A_1 and A_3 deduced for Ti_2O_3 from our 77-K data to calculate piezoresistances for other temperatures by means of Eqs. (7) and (8). The results are shown as the solid curves in Figs. 1 and 2. Good fits to the data were obtained, except near 300 K, where the minor effects presumably become relatively more important. In addition, the process which causes piezoresistance extrema at higher temperatures³¹ may have started to make an appreciable contribution.

The 77-K values of A_i 's were also used to calculate the piezoresistance for the case of uniaxial compression and current parallel to the $[001]$ and $[01\bar{1}]$ directions and for the case of hydrostatic pressure. The pertinent relations deduced from the simple, two-band deformation potential model are

$$\begin{aligned} (\Delta\rho/\rho_0|X|)_{[01\bar{1}+1]} \\ = -[A_1(S_{11} + S_{12} + 2S_{13}) + A_3(S_{13} + S_{33})]/4kT \end{aligned} \quad (9)$$

and

$$\Delta\rho/\rho_0|P| = -[2A_1(S_{11} + S_{12} + S_{13}) + A_3(2S_{13} + S_{33})]/2kT. \quad (10)$$

The curve calculated by means of Eq. (9) is shown in Fig. 3. It lies below the data by amounts which appear to be much larger than those occurring for a - and c -length samples. (See Figs. 1 and 2.) Part of the reason for this is the larger scale used in Fig. 3. In addition, because of the smallness of the uniaxial piezoresistances for $[011]$ and $[01\bar{1}]$ samples, contributions from any minor effects will be relatively more important. The curve calculated using Eq. (10) agrees well with data (see Fig. 4.), even though the magnitude of $\Delta\rho/\rho_0|P|$ is relatively small. This may be due to the smaller likelihood of minor effects occurring for hydrostatic than for uniaxial stress.

The good agreement between the calculated curve and the data for the case of hydrostatic pressure confirms that reduction in the concentrations of mobile charge carriers continues unabated well below room temperature without any indication of an approach to extrinsic behavior, as occurs, for

example, in p -type InSb.³⁷ A continuing decrease in carrier concentration with decreasing temperature is, of course, the simplest way to interpret the resistivity-versus-temperature data of others^{5,6} and ours. The main reason for questioning the intrinsic character of Ti_2O_3 is that the amount by which the resistivity changes at the electrical transition is somewhat sample dependent.³⁸ A secondary reason is that at temperatures just below the transition range the log of the resistivity rises less rapidly than it does at lower temperatures. This effect could, of course, be due to the mobility rising appropriately as T decreases in a limited temperature range as previous work has indicated⁴ or implied.⁶

It should be emphasized that the fact that $\Delta\rho/\rho_0P$ is proportional to $1/T$ precludes interpreting the approximately $1/T$ dependence of the uniaxial piezoresistances as being due to the transfer of carriers between different valleys of a multivalley band or between different regions of an anisotropic or warped energy band.²⁰ The reason is that, unlike uniaxial stress, hydrostatic pressure does not alter crystal symmetry, and hence cannot remove symmetry degeneracies in the band structure or change the shape of the energy bands.

IV. CONCLUSION

Our piezoresistance results indicate that the valence- and conduction-band edges in semiconducting Ti_2O_3 are describable in terms of two simple bands located on the k_z axis and that stress changes only the separation between the bands (i.e., a deformation potential model is applicable). Thus we have found no evidence for complexities in the band edges like those implied by the band calculation of Ashkenazi and Chuchem.¹⁴

The dependence of the resistivity on uniaxial compression is consistent with the way it is correlated with changes in lattice parameters at the semiconductor-to-semimetal transition (between about 400 and 550 K). This provides presumptive evidence that band shift rather than band broadening is involved in the transition.

ACKNOWLEDGMENTS

Thanks are due to Professor W. M. Becker, Dr. R. Y. Sun, and K. Hu for use of some apparatus and assistance with the frozen-fluid bomb technique.

- †Work supported by Purdue Research Foundation David Ross Grant and NSF Grant Nos. DMR 72-03018A03 (MRL Program) and DMR 72-03012A2.
- ¹See, for example, R. E. Newnham and Y. M. Dehaan, *Z. Kristallogr.* **17**, 235 (1962), or W. R. Robinson, *J. Solid State Chem.* **9**, 225 (1974).
- ²A. D. Pearson, *J. Phys. Chem. Solids* **5**, 316 (1958).
- ³F. J. Morin, *Phys. Rev. Lett.* **3**, 34 (1959).
- ⁴J. Yahia and H. P. R. Frederikse, *Phys. Rev.* **123**, 2357 (1961).
- ⁵J. M. Honig and T. B. Reed, *Phys. Rev.* **174**, 1020 (1968).
- ⁶S. H. Shin, G. V. Chandrashekhar, R. E. Loehman, and J. M. Honig, *Phys. Rev. B* **8**, 1364 (1973).
- ⁷J. B. Goodenough, *Phys. Rev.* **117**, 1442 (1960).
- ⁸L. L. Van Zandt, J. M. Honig, and J. B. Goodenough, *J. Appl. Phys.* **39**, 594 (1968).
- ⁹J. B. Goodenough, in *Proceedings of the Tenth International Conference on the Physics of Semiconductors, Cambridge, Mass., 1970*, edited by S. P. Keller, J. C. Hensel, and F. Stern (U.S. AEC Division of Technical Information, Oak Ridge, Tenn., 1970), p. 304.
- ¹⁰H. J. Zeiger, T. A. Kaplan, and P. M. Raccach, *Phys. Rev. Lett.* **26**, 1328 (1971).
- ¹¹H. J. Zeiger, *Phys. Rev. B* **11**, 5132 (1975).
- ¹²N. F. Mott and L. Friedman, *Phil. Mag.* **30**, 389 (1974).
- ¹³I. Nebenzahl and M. Weger, *Phil. Mag.* **24**, 1119 (1971).
- ¹⁴J. Ashkenazi and T. Chuchem, *Phil. Mag.* **32**, 763 (1975).
- ¹⁵D. W. Fischer and W. L. Baun, *J. Appl. Phys.* **39**, 4757 (1968).
- ¹⁶S. H. Shin, F. H. Pollak, T. Halpern, and P. M. Raccach, *Solid State Commun.* **16**, 687 (1975).
- ¹⁷See, for example, A. C. Beer, in *Solid State Physics*, edited by F. Seitz and D. Turnbull (Academic, New York, 1966), Suppl. 8.
- ¹⁸J. M. Honig, L. L. Van Zandt, T. B. Reed, and J. Sohn, *Phys. Rev.* **182**, 863 (1969).
- ¹⁹J. Dumas and C. Schlenker, *J. Phys. (Paris)* **37**, C4-41 (1976).
- ²⁰R. W. Keyes, in *Solid State Physics*, edited by F. Seitz and D. Turnbull (Academic, New York, 1960), Vol. 11, p. 149.
- ²¹C. S. Smith, in *Solid State Physics*, edited by F. Seitz and D. Turnbull (Academic, New York, 1958), Vol. 8, p. 175.
- ²²T. B. Reed, R. E. Fahey, and J. M. Honig, *Mater. Res. Bull.* **2**, 561 (1967).
- ²³L. W. Lonney, Jr., M. S. Thesis, Purdue University, 1970 (unpublished).
- ²⁴R. J. Sladek, *Phys. Rev.* **140**, A 1345 (1965).
- ²⁵R. Y. Sun, Ph.D. thesis (Purdue University, 1974) (unpublished).
- ²⁶T. C. Chi and R. J. Sladek, *Phys. Rev. B* **7**, 5080 (1973).
- ²⁷R. W. Keyes, *J. Electron. Control* **2**, 279 (1956).
- ²⁸B. Visivanathan, S. Usha Devi, and C. N. R. Rao, *Pramana* **1**, 48 (1973).
- ²⁹C. Herring, *Bell. Syst. Tech. J.* **34**, 237 (1955).
- ³⁰J. G. Bennett and R. J. Sladek, *IEEE Proc.* **74**, CHO 896-ISU 517 (1974).
- ³¹H.-L. S. Chen and R. J. Sladek, *Bull. Am. Phys. Soc.* **21**, 437 (1976).
- ³²C. E. Rice and W. R. Robinson, *Mater. Res. Bull.* **11**, 1355 (1976).
- ³³L. Kleinman, *Phys. Rev.* **128**, 2614 (1962); **130**, 2283 (1963); **132**, 1080 (1963).
- ³⁴A. L. Jain and R. Jaggi, *Phys. Rev.* **135**, A708 (1964).
- ³⁵See, for example, R. T. Bate, W. E. Drobish, and N. G. Einspruch, *Phys. Rev.* **149**, 485 (1966).
- ³⁶See, for example, J. J. Hall and S. H. Koenig, *IBM J. Res. Develop.* **8**, 241 (1964).
- ³⁷A. Tuzzolino, *Phys. Rev.* **109**, 1980 (1958).
- ³⁸This is deducible by comparing results of various authors, including those of Refs. 2, 3, 5, and 6 and of others cited therein. The most pertinent comparison is between Refs. 5 and 6, because of the generally improved and similar sample quality in them.